

Optical Properties and Determination of Thermal Transformation Parameters for $\text{Se}_{0.65}\text{Te}_{0.35}$ High Reflectance Thin Films

Ayman Ahmed EL-AMIN, Aly Mohammed BADR, Foad ABDEL-WAHAAB
Physics Department, Faculty of Science, South Valley University, Aswan-EGYPT
e-mail: badr_egsc@yahoo.com

Received 19.04.2007

Abstract

Chalcogenide glasses Se-Te have been prepared from the high purity constituent elements. Thin films of these materials have been deposited by vacuum evaporation. The thickness effects on the optical properties have been performed for the as-deposited films. The impact of varying thickness on the value of the optical gap is also reported and discussed. The resultant films were in amorphous nature. The reflectance and transmittance spectra were measured for the mentioned films and analyzed in the incident photon energy range from 1.16 to 2.47 eV. The refractive indices were determined as a function of wavelength via the transmittance analysis in the incident photon energy range from 1.16 to 1.38 eV. Also, the dispersion energy, oscillator energy, static refractive index and static dielectric constant were calculated for the thicknesses under investigation. The results of differential scanning calorimetry (DSC) at different heating rates are reported and analyzed. The activation energies for the glass transition and crystallization were calculated.

Key Words: Optical Properties and Parameters; High Reflectance Chalcogenide Semiconductors; Thermal Transformation Parameters.

1. Introduction

Studies on semi-conducting Chalcogenides glasses have received much attention due to their important optical applications in IR region [1, 2]. Effect of impurities on chalcogenide materials may have an importance in the fabrication of amorphous semiconductor devices. The most important applications of chalcogenides are now in the field of optics and arise mainly from either their exhibited infrared transmitting properties or photo-induced effects. They have potential uses in integrated optics, optical imaging, optical data storage and infrared optics [3-6]. The structure of the thin films strongly influences the electronic properties and is highly dependent upon the preparation technique and deposition conditions [7]. Se-Te alloys have gained much attention and found to be useful in practical application [8]. Technologically, these glasses should be thermally stable. Thus differential scanning calorimetry was used in order to investigate the characteristic temperatures such as glass, crystallization and melting temperatures. The optical band gap, refractive index and extinction coefficient are the most significant parameters in the amorphous semi-conducting thin films. And, accurate measures of a material's optical character can be revealed in its thin films [9].

Chalcogenide materials were found to exhibit change in refractive index under the influence of light, which makes it possible to use these materials to record not only magnitude but also phase of illumination. The later is important especially in holographic optical data storage and in the fabrication of various integrated components and devices such as selective optical fiber, mixers, couplers and modulators [10]

The objective of this work is to elucidate the optical and thermal properties of the $\text{Se}_{0.65}\text{Te}_{0.35}$ amorphous thin films followed by their discussion and analyses. Samples used in this work were chosen in a thickness range whose variation influences the optical properties and parameters.

2. Experimental Setup

Thermal evaporation technique is used for obtaining six thicknesses of $\text{Se}_{0.65}\text{Te}_{0.35}$ amorphous thin films. Under this method, starting compounds are evaporated and collimated under vacuum ($\sim 10^{-6}$ torr) onto cleaned glass substrates. Starting materials were powders in amorphous state. The glass substrates were, sequentially, carefully cleaned using hot water, NaOH solution, chromic acid, distilled water and isopropyl alcohol. Thermal evaporation was undertaken using a Edwards E306A coating unit. The unit has attached its own two-stage rotary pump/diffusion pump system. For each sample under preparation, a molybdenum boat is charged with the starting compounds in granular form and stoichiometric ratio, and the vacuum chamber is pumped down to about $\sim 10^{-6}$ torr. Under a shutter, the boat is gradually heated until the contain material starts to evaporate. At this point the shutter is removed, allowing the vapor to coat the glass substrates. The X-ray diffraction patterns exhibit no intense peaks that indicate these films are of amorphous nature. A Shimadzu model UV-1650PC UV-visible double beam spectrophotometer is employed to record the reflectance and transmittance spectra over the incident photon energy of the wavelength range from 500 to 1060 nm. From these spectra, the absorption coefficient, extinction coefficient and refractive index are determined. 15 mg powdered samples from each of the as-prepared bulk specimens were examined using a TA Instruments model DSC-2010 differential scanning calorimeter under pure nitrogen atmosphere. A complete set of DSC thermograms was obtained. These DSC thermograms were measured at different heating rates, from 5 to 20 K/min.

3. Results and Discussion

3.1. Optical properties

Figure 1 shows the transmittance of the $\text{Se}_{0.65}\text{Te}_{0.35}$ amorphous thin films. Optical band gaps estimated in each thin film from transmittance and reflectance spectra were constant across thicknesses above $0.1 \mu\text{m}$ and thus are excluded from the present discussion. Instead, six thickness less than $0.1 \mu\text{m}$ have been chosen. Note the similar behavior for thicknesses from 47.9 to 83.5 nm in the incident photon energy region of the wavelength range from 500 to 1060 nm (see Figure 1). This figure shows that, with increase in thickness, there is a shift in transmittance toward regions of shorter wavelength. The shift may be influenced by the superposition degree of the electron clouds of the neighboring atoms, which consequently affect the optical band gap width.

One can predict that the obtained films have a high reflectance and the reflectance decreases with increased thickness. Interaction of the incident light with the thin films is analyzed in three parts: transmitted light, absorbed and reflected parts, for which representative data is shown in Figures 1, 2 and 3, respectively.

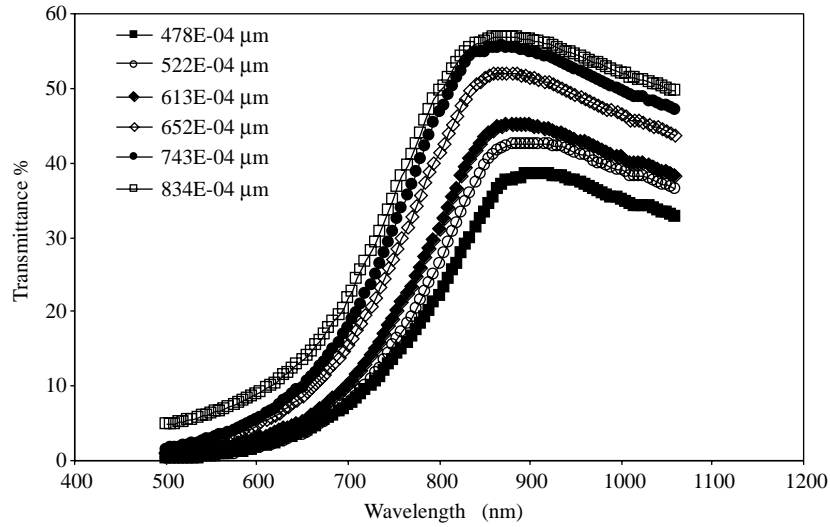


Figure 1. Transmittance spectra of the amorphous $\text{Se}_{0.65}\text{Te}_{0.35}$ thin films.

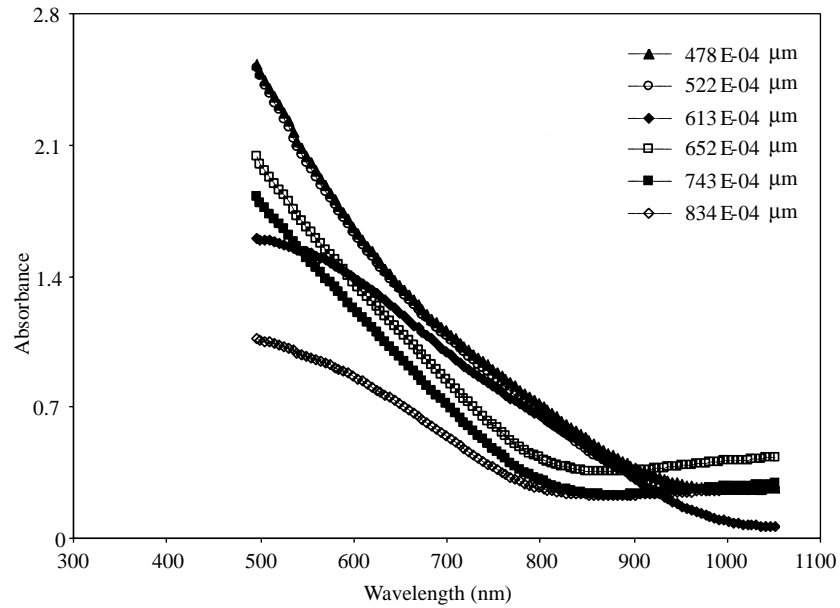


Figure 2. Absorbance of the amorphous $\text{Se}_{0.65}\text{Te}_{0.35}$ thin films.

As it is known, optical measurements are productive tools for understanding band structure and the energy gap width of both crystalline and amorphous non-metallic materials. The optical absorption coefficient α is related to the transmittance T of a sample with thickness d through the relation

$$\alpha = \frac{2.303}{d} \log \left(\frac{1}{T} \right). \quad (1)$$

According to reference [11], it is possible to separate three distinct regions in the absorption edge spectrum of amorphous semiconductors. The first is the weak absorption tail, which originates from defects and impurities. (Existence of the weak absorption tails in the band gaps of the films under study may be attributed to the amorphous nature of, and randomly distributed impurities in the films [12].) Second is the exponential edge region, which is strongly related to the structural randomness of the amorphous compound. Third is the high absorption region from which optical energy gap width can be determined. The above

three absorption regions can easily observed in Figure 2, where these regions are different in their beginnings and endings for the different thicknesses under investigation.

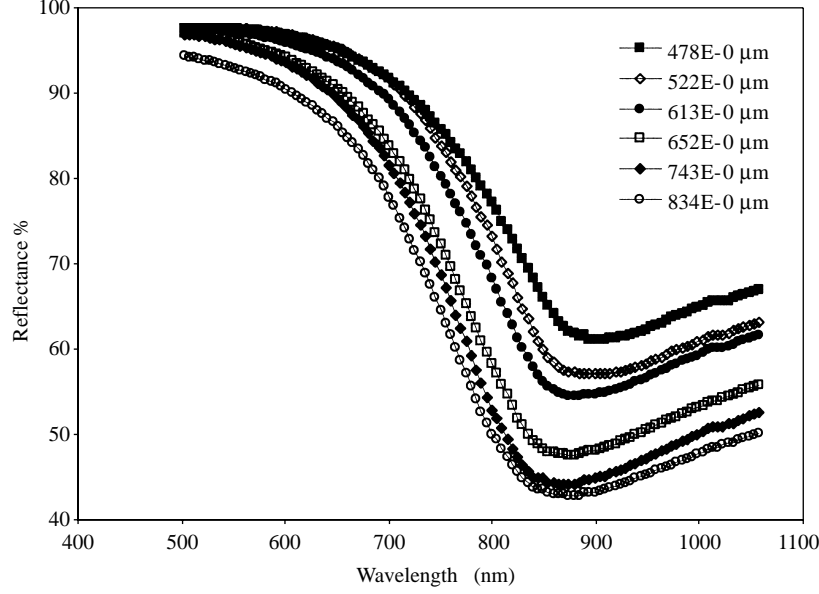


Figure 3. Reflectance spectra of the amorphous $\text{Se}_{0.65}\text{Te}_{0.35}$ thin films.

In the high absorption regions (linear increase in α with increase in incident photon energy), the relationship between the absorption coefficient and the incident photon energy is governed by the relation [13, 11]

$$\alpha = \frac{B (h\nu - E_g)^n}{h\nu}, \quad (2)$$

where B is a constant that depends on the transition probability, E_g is the width of the band gap, and n is an index that characterizes the optical absorption processes in amorphous $\text{Se}_{0.65}\text{Te}_{0.35}$ thin films. Analysis of experimental results showed that a proportionality is revealed between the absorption coefficient and the frequency of the photon energy in the form $(h\nu - E_g)^n$. The exponent n can take one of the four values: 2, 1/2, 3 and 3/2, which define the type of the optical transition. Theoretically n is equal to 2, 1/2, 3 or 3/2 for the indirect allowed, direct allowed, indirect forbidden and direct forbidden transitions, respectively [14]. On other hand, the usual method for determining the type of optical transition includes plots of $(\alpha h\nu)^{1/n}$ as a function of incident photon energy $h\nu$. These proportionalities give a set of plots with four values of the exponent n : $(\alpha h\nu)^{1/2} - h\nu$, of $(\alpha h\nu)^2 - h\nu$, of $(\alpha h\nu)^{1/3} - h\nu$ and of $(\alpha h\nu)^{2/3} - h\nu$. One of these plots satisfies the widest linearity of data, and hence its exponent determines the type of the optical transition. In the present study, values of n indicate that the dominant transition is direct-allowed. A plot of $(\alpha h\nu)^2$ as a function of $h\nu$ is shown in Figure 4. In this work, the optical band gaps were calculated by linear fitting in the high absorption regions. These fits intersect the $h\nu$ -axis at the values of the optical band gap widths, and show that the direct allowed band gap width of the amorphous $\text{Se}_{0.65}\text{Te}_{0.35}$ thin films decreases with the increase in the film thickness (see Table 1).

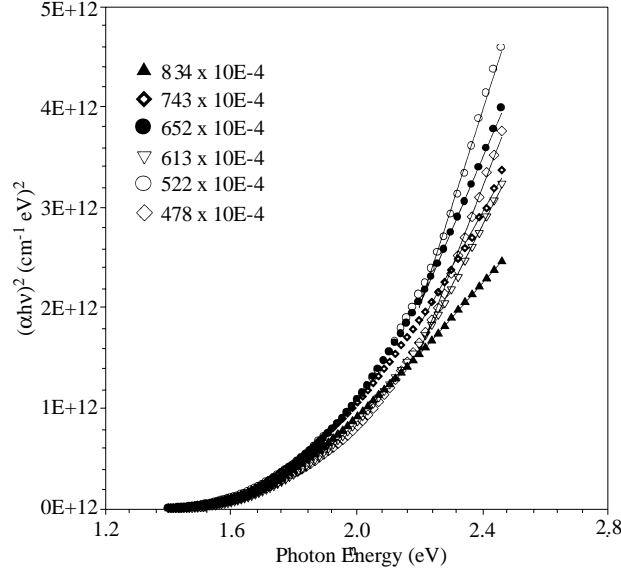


Figure 4. Plot of $(\alpha hv)^2$ as a function of hv .

The refractive index n can be calculated using the relation [15]

$$R = \frac{(n - 1)^2 + k^2}{(n + 1)^2 + k^2}, \tag{3}$$

where k is the extinction coefficient. Relation (3) can be rewritten for the transparent range of irradiance in the form

$$R = \left(\frac{n - 1}{n + 1} \right)^2. \tag{4}$$

Figure 5 shows the points that represent the calculated values of the refractive index in the incident photon energy region 1.16 to 1.38 eV. It is evident from this figure that the dispersion of the refractive index is normal for all the thicknesses under investigation and can be well described using a single oscillator model [16]:

$$n^2 = 1 + \frac{E_o E_d}{E_o^2 - (hv)^2} \tag{5}$$

$$\Rightarrow (n^2 - 1)^{-1} = \frac{E_o}{E_d} - \left(\frac{1}{E_o E_d} \right) (hv)^2, \tag{6}$$

where, E_o is the single oscillator energy, E_d is the dispersion energy, and hv is the incident photon energy. It is observed from Figure 5 that the refractive indices of the thicknesses under investigation vary linearly with variation of the incident photon energy in the region 1.36 to 1.75 eV. Both the single oscillator energy E_o and is the dispersion energy E_d can be obtained for all mentioned thicknesses by plotting $(n^2 - 1)^{-1}$ as functions of the photon energy hv in the linear region of the n - λ plots (from 1.36 to 1.75 eV). The $(n^2 - 1)^{-1}$ versus $(hv)^2$ in the mentioned linear region is illustrated in Figure 6. The E_d and E_o were calculated from the slope $(E_o E_d)^{-1}$ and the intercept (E_o/E_d) . The values of oscillator energies E_o , dispersion energies E_d , and optical band widths E_g for the six thicknesses under investigation of $Se_{0.65}Te_{0.35}$ amorphous thin films are summarized in Table 1.

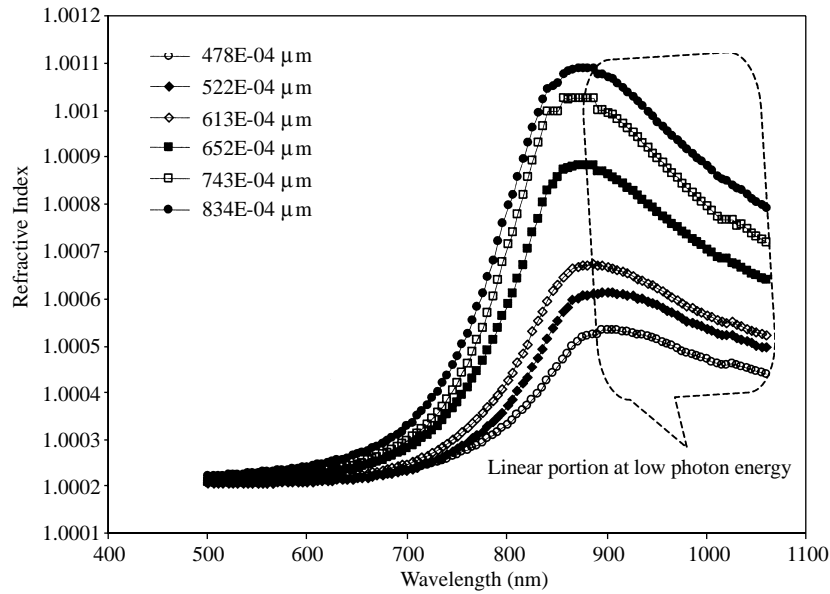


Figure 5. Dependence of refractive index n on the incident photon energy.

Both Figure 6 and the calculated values recorded in Table 1 suggest an overall decrease in the oscillator energies E_o with the increase in thickness of amorphous $\text{Se}_{0.65}\text{Te}_{0.35}$ thin films, but the dispersion E_d of the refractive index nearly increases as the thickness decreases. By using Figure 4 the values of the optical band gap width are calculated for all the six thicknesses under study. These values are plotted in Figure 7, which shows decrease in the optical band gaps of amorphous $\text{Se}_{0.65}\text{Te}_{0.35}$ thin films with increasing the thickness from 47.8 to 83.4 nm. A similar behavior has been obtained by Sharma and Katyal for Ge-Se-Te system [17]. The variation of the optical band gap for the mentioned thicknesses of amorphous $\text{Se}_{0.65}\text{Te}_{0.35}$ thin films are recorded in Table 1.

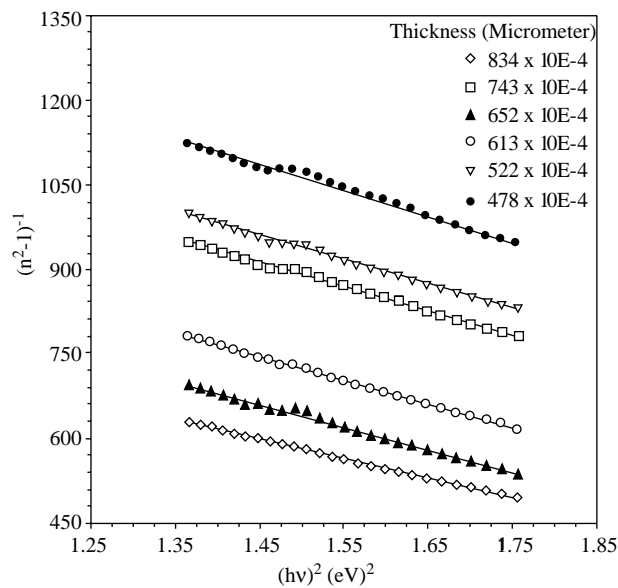


Figure 6. Plot of $(n^2 - 1)^{-1}$ as a function of $(hw)^2$

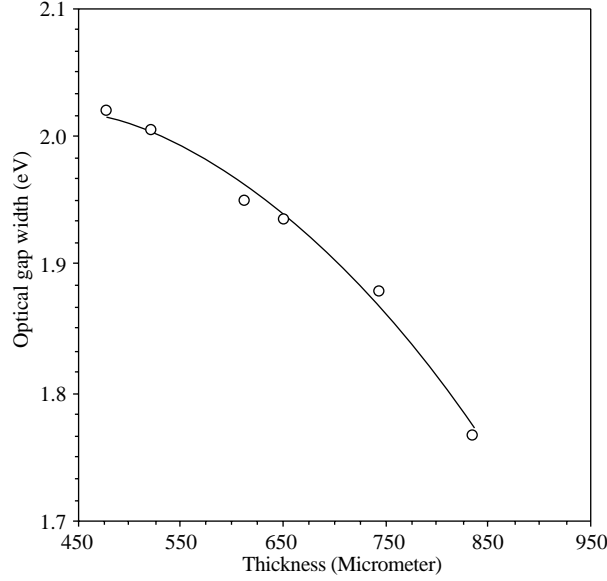


Figure 7. Dependence of the direct band gap on thickness.

Table 1. The optical parameters of different thicknesses.

Thickness (nm)	Oscillator Energy E_0 (eV)	Dispersion Energy E_d (meV)	Optical band width E_g (eV)
47.8	1.97	1.14	2.02
52.2	1.91	1.20	2.00
61.3	1.8	1.34	1.95
65.2	1.76	1.42	1.93
74.3	1.88	1.22	1.88
83.4	1.79	1.63	1.77

3.2. Thermal properties

Non-isothermal conditions was performed on 15 mg of the powdered samples from the as prepared bulk specimens with continuous heating rates (β) ranging from 5 to 20 K/min. Figure 8 shows a set of DSC thermograms of the powdered samples from the as-prepared bulk specimens. These thermo-grams were observed in the above mentioned figures at different heating rates β from 5 to 20 K/min. It is clear that the three characteristic temperatures increased with increasing the heating rate.

The dependence of T_g on the heating rate can be view via two approaches. The first relates T_g to β in the form [18]

$$T_g = A + B \ln(\beta), \tag{7}$$

where A and B are constants. The constant B indicates the response of the configuration within the glass transition region to the heating rate. Figure 9 shows a relation between the characteristic temperatures and $\ln(\beta)$. The values of A and B were extracted from the straight line segments of Figure 9 and are found to be ~ 62.01 and ~ 7.04 , respectively. The second approach is due to Kissinger [19] and is expressed in the form

$$\ln\left(\frac{T_g^2}{\beta}\right) = \frac{E_g}{RT_g} + C, \tag{8}$$

where E_g is the activation energy of glass transition for homogeneous crystallization with spherical nuclei, and C is a constant. For the present sample and with the aid of equation 8, the values of E_g and C were calculated to be ~ 119 kJ/mol and 1.4×10^4 , respectively.

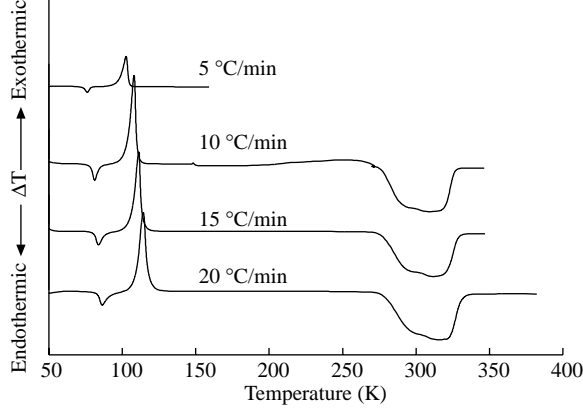


Figure 8. DSC thermograms measured at different heating rates.

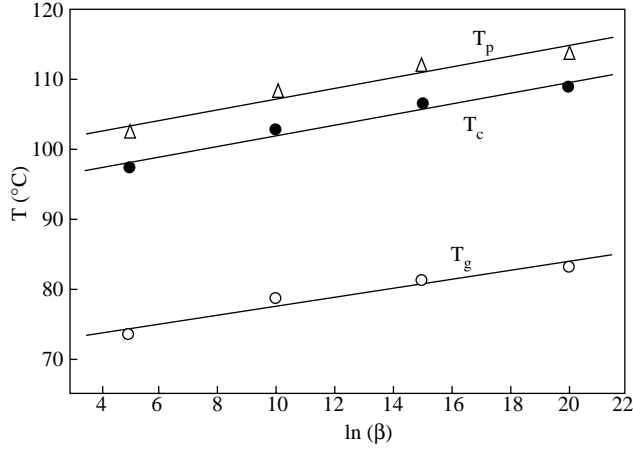


Figure 9. Relation between the characteristic temperature and continuous heating rates.

The glass transition temperature of the present sample increases as heating rate increased. This phenomenon may be explained in terms of glass formation thermodynamics. It should be mentioned again the sample was prepared by melt quenching, i.e. the rate of cooling was several hundred degrees in a few second. When analyzed with different heating rates, the difference between the reheating rate and the cooling rate is not equal, indicating the structure is different between the cooled liquid and reheated solid. On the other hand the variation of T_C with heating rate allowed us to calculate the activation energy of crystallization E_C .

The value of E_c can be deduced by two methods, first from the following relation [20]:

$$\ln(\beta) = -\left(\frac{E_C}{RT_C}\right) + constant. \tag{9}$$

Also using the approximation method developed by Augis and Bennett [21], the activation energy can be determined the relation used by them is

$$\ln\left(\frac{\beta}{T_C}\right) = -\left(\frac{E_C}{RT_C}\right) + \ln K_0. \tag{10}$$

The activation energy of crystallization that evaluated respectively by the two methods are 142 kJ/mol and 139 kJ/mol. This is lower than the value obtained by Afify et al [22] for $Se_{0.65}Te_{0.35}$ (161.7 kJ/mol)

Conclusion

In accordance with the optical measurements, it was found that, for the $\text{Se}_{0.65}\text{Te}_{0.35}$ thin films with thicknesses greater than $0.1 \mu\text{m}$, optical band gap and optical parameters did not depend on thickness. The transition type in amorphous $\text{Se}_{0.65}\text{Te}_{0.35}$ thin films exhibit direct allowed. For thicknesses down to $\sim 0.1 \mu\text{m}$, the band gap widths were calculated and found to decrease with increase in film thickness. Variations of refractive indices were calculated and found to decrease with increase in thickness. Via optical measurements, both the oscillator E_o and dispersion E_d energies of the refractive index were calculated. Non-isothermal conditions was performed on 15 mg of the powdered samples from the as prepared bulk specimens with continuous heating rates (α) ranging from 5 to 20 K/min. A complete set of DSC thermograms, measured at different heating rates from 5 to 20 K/min, was generated from powdered samples of as-prepared bulk specimens. Values of the transformation parameters, such as the glass-transition temperature T_g , the onset crystallization temperature T_c and the peak crystallization temperature T_p were evaluated. The glass transition of the $\text{Se}_{0.65}\text{Te}_{0.35}$ activation energy E_t of the structural relaxation was calculated to be 119 kJ/mol, however the crystallization activation energy was determined to be approximately 142 kJ/mol.

References

- [1] A. R. Hilton, D. J. Hayes and M. D. Rechitin, *J. Non-Cryst. Solids*, **17**, (1975), 319.
- [2] A. Vasko, in: *Proceedings of the 11th international congress on glass*, **5**, (1977), Prague, 533.
- [3] J. S. Sanghara and I. D. Agarwal, *J. Non-Cryst. Solids*, **6**, (1999), 256.
- [4] K. Schwarts, *The Physics of Optical Recording*, (Berlin, Springer-Verlag. 1993).
- [5] A. Pradley, *Optical Storage for Computers Technology and Applications*, (Ellis Horwood Limited, New York. 1989).
- [6] K. L. Tai, E. Ong and R. G. Vadimsky, *Proc. Electro. Chem. Sci.*, **9**, (1982), 82.
- [7] Pathinettan Padiyan, A. Marikani and K. R. Murali, *Cryst. Res. Technol.*, **35**, (2000), 949.
- [8] A. H. Moharram, *Thin Solid Films*, **392**, (2001), 34.
- [9] V. Pandey, N. Mehta, S. K. Tripathi and A. Kumer, *Chalcogenide Letters*, **2**, (2005), 39.
- [10] V. Pandey, N. Mehta, S. K. Tripathi and A. Kumar, *Chalcogenide Letters*, **2**, (2005), 39.
- [11] J. Tauc, *Amorphous and Liquid Semiconductors*, (New York, Plenum. 1974), Ch. 4.
- [12] V. N. Chernyaev and V. F. Korzo, *Thin Solid Films*, **37**, (1976), L61.
- [13] J. I. Pankove, *Optical processes in Semiconductors*, (New Jersey, Prentice-Hall. 1971), p. 93.
- [14] A. F. Qasrawi, *Cryst. Res. Technol.*, **40**, (2005), 610.
- [15] J. I. Pankove, *Optical process in semiconductors*, (Prentice Hall Inc., 1971), p. 45.
- [16] C. Baban, G. I. Rusu and P. Prepelita, *Journal of Optoelectronics and Advanced Materials*, **7**, (2005), 817.
- [17] P. Sharma and S. C. Katyal, *Mater. Lett.*, **61**, (2007), 4516.
- [18] M. Lasocka, *Mater. Sci. Eng.*, **23**, (1976), 173.
- [19] H. E. Kissinger, *J. Res. Natl Bur. Stand.*, **57**, (1956), 217.
- [20] T. Ozawa, *J. Therm. Anal.*, **2**, (1970), 301.
- [21] J. A. Augis, J. E. Bennett, *J. Them. Anal.*, **13**, (1978), 283.
- [22] N. Afify, A. Gaber, I. Abdalla and H. Talaat, *Physica B*, **229**, (1997), 167.